Polymer Chemistry

Sub-10 nm Domains in High-performance Polyetherimides

Journal:	*Polymer Chemistry*
Manuscript ID	PY-ART-10-2018-001460.R1
Article Type:	Paper
Date Submitted by the Author:	30-Nov-2018
Complete List of Authors:	Guo, Dong; Virginia Polytechnic Institute and State University, Khan, Assad Ullah; Virginia Polytechnic Institute and State University, Chemistry; Liu, Tianyu; Virginia Polytechnic Institute and State University, Department of Chemistry Zhou, Zhengping; Virginia Polytechnic Institute and State University, Chemistry Liu, Guoliang; Virginia Polytechnic Institute and State University, Department of Chemistry

Journal Name

ARTICLE

Sub-10 nm Domains in High-Performance Polyetherimides

Dong Guo,[a] Assad U. Khan,[a] Tianyu Liu,[a] Zhengping Zhou[a] and Guoliang Liu*[abc]

Received 00th January 20xx,
Accepted 00th January 20xx

DOI: 10.1039/x0xx00000x

www.rsc.org/

Dielectric polyetherimide (PEI) thin films require ultra-small air voids to reduce the dielectric constant and maintain the structural integrity. Conventional synthesis of dielectric PEI uses thermally labile high-molecular-weight polymers to create air voids. The air voids, however, range from hundreds of nanometers to several micrometers, which limits the use of PEI in ultrathin films. Herein we present the synthesis of polystyrene-*b*-polyetherimide-*b*-polystyrene (PS-*b*-PEI-*b*-PS) triblock copolymers with ultra-low molecular weights. The molecular weights of the thermally labile polystyrene (PS) blocks are controlled to be as low as 1.5 kDa. By tuning the molecular weight of the PEI block to be 8, 10, and 12 kDa, the volume fractions of PS are 30.4%, 26.4%, and 23.4%, respectively. The triblock copolymers exhibit PS nanostructures of < 8 nm in size. Such small domains will potentially enable the preparation of ultra-small air voids in PEIs.

Introduction

Polyetherimide (PEI) is a class of polyimides that have low dielectric constant, high mechanical strength, flame retardancy, chemical resistance, and good processibility.[1-5] Owing to these outstanding properties, PEIs are promising low-κ dielectric polymers in microelectronics.[6] To further reduce the dielectric constant of PEIs, there are generally two strategies. One is to incorporate alicyclic structures[6, 7] or fluorine groups[8, 9] to increase the free volume in the PEIs. The other is to synthesize PEI-based block copolymers which consist of low dielectric or thermally labile peripheral blocks. The latter is attractive due to the simplicity of preparing the monomers. After forming the block copolymer nanostructures, the labile blocks are often removed via thermolysis to produce air voids or pores (κ~1) in the polyimide matrix and reduce the overall dielectric constant.[10-22] The synthesis of dielectric polymers with ultra-small thermally labile blocks, however, has been the key challenge.

To maintain the structural integrity of porous PEI thin films, the pore size must be significantly smaller than the thickness of the films. The inclusion of porous structures in polyimides has been successful, notably when the pore size is in the 100 nm region.[13, 14, 17, 21, 22] Many researchers have produced porous polyimides with the pore size even up to several micrometers.[10-12, 15, 16, 18-20] The large pore sizes are due to the large molecular weights of the thermally labile blocks. In terms of the polymer composition, various thermally labile polymers were employed to react with polyimides, for example, polystyrene (PS),[14] poly(methyl methacrylate),[10, 17] poly(propylene oxide),[12, 13, 20] poly(ε-caprolactone),[15, 16, 21] poly(ethylene glycol),[18] and poly(α-methyl styrene).[11, 19, 22] Among the thermally labile polymers, PS is the most attractive because it has a slow decomposition rate and minimizes the generation of "blowing agents".[14] Other polymers such as poly(α-methyl styrene) generate "blowing agents" that plasticize the matrix polymer and detrimentally increase the pore sizes.[11, 19, 22] The large pores, however, limit the preparation of extremely thin dielectric polymer films. Therefore, it is highly desirable to synthesize PS and PEI-based block copolymers, in which the thermally labile PS blocks have ultra-low molecular weights but maintain the capability of forming nanoscale domains in the PEI matrix.

Herein we establish a synthetic route for polystyrene-*b*-polyetherimide-*b*-polystyrene triblock copolymers (PS-*b*-PEI-*b*-PS, abbreviated as SIS). We also demonstrate the formation of ultra-small thermally labile domains by utilizing the disordered nanostructures of block copolymers. The SIS triblock copolymers were prepared by reacting anhydride-terminated telechelic PEI (PEI-DA) with amine-terminated PS oligomers. The volume fractions of the PS blocks were controlled to be 23.4%, 26.4%, and 30.4% by changing the molecular weight of PEI-DA but keeping PS at a constant molecular weight of 1.5 kDa. Due to the low molecular weight of PS, the SIS triblock copolymers exhibited disordered nanostructures after thermal annealing at temperatures above the glass transition temperatures of both blocks, leading to ultra-small PS domains embedded in the PEI matrix. The average dimension of the PS domains was less than 8 nm and the nanostructures exhibited

[a] *Department of Chemistry, Virginia Tech, Blacksburg, Virginia 24061, United states*
[b] *Macromolecules Innovation Institute, Virginia Tech, Blacksburg, Virginia 24061, United states*
[c] *Division of Nanoscience, Virginia Tech, Blacksburg, Virginia 24061, United states*
† E-mail: gliu1@vt.edu
Electronic Supplementary Information (ESI) available: [details of any supplementary information available should be included here]. See DOI: 10.1039/x0xx00000x

semi-periodic spacings of 14.1-15.2 nm, showing great promise of preparing PEI thin films with ultra-small porous structures.

Experimental

Materials

2,2-bis[4-(3,4-dicarboxyphenoxy)phenyl]propane dianhydride (BPADA) was dried by one heating-cooling cycle between room temperature (RT) and 200 °C prior to use. *m*-Phenylenediamine (mPD, Sigma-Aldrich) was purified by sublimation. Styrene, *N,N,N′,N″,N‴*-pentamethyldiethylenetriamine (PMDETA), *o*-dichlorobenzene (oDCB), copper(I) chloride (CuCl), phthalic anhydride, 3-phenylpropylamine, *N*-bromosuccinimide (NBS), benzoyl peroxide (BPO), sodium sulphate, carbon tetrachloride (CCl_4), dioxane, dichloromethane (DCM), toluene, tri-*n*-butyltin hydride, azobisisobutyronitrile (AIBN), hydrazine solution (1 M) in tetrahydrofuran (THF), and ninhydrin reagent N7285 were used as received from Sigma-Aldrich.

Synthesis of 2-(3-bromo-3-phenylpropyl)isoindoline-1,3-dione (BPI)

BPI was synthesized according to a report by Pourjavadi *et al*.[23] and used as the initiator for the polymerization of PS. Briefly, 3-phenylpropylamine (4.1 g, 30 mmol) and phthalic anhydride (4.4 g, 30 mmol) were mixed in a 250-mL round-bottom flask. The mixture was heated at 120 °C for 1 h under constant agitation by a magnetic stirring bar. The viscous mixture was cooled to RT and dissolved in 15 mL of DCM. The DCM solution was then transferred to a separatory funnel. After addition of 15 mL of deionized water and vigorous agitation, the bottom portion, *i.e.*, the DCM phase, was extracted. The extraction was repeated three times. The resulting DCM solution was dried using anhydrous sodium sulphate. After the evaporation of DCM using a rotary evaporator, a yellowish powder was collected and dried *in vacuo*. A portion of the yellow powder (1.0 g, 3.8 mmol), NBS (0.71 g, 4.0 mmol), and BPO (0.020 g, 0.083 mmol) were dissolved in 20 mL of CCl_4 and refluxed at 85 °C overnight in a 100-mL round-bottom flask. After cooling down to RT and subsequent filtration, the filtrate was collected and CCl_4 was removed using a rotary evaporator, resulting in another yellow powder. After drying at RT overnight *in vacuo*, the powder was further purified by column chromatograph using silica gel (200-425 mesh) and an eluent composed of hexane and DCM with a volumetric mixing ratio of 1:1. The retention factor (Rf) was ~0.5. Finally, white crystals of BPI were obtained after evaporating the eluent and drying at RT overnight *in vacuo*. The yield of BPI was ~85%.

Synthesis of phthalimido-polystyrene-Br (PTA-PS-Br)

Following the synthesis in a previous report,[24] 5 mL of styrene (with inhibitor removed by aluminium oxide chromatography) and PMDETA (0.43 g, 2.4 mmol) were dissolved in 10 mL of dioxane in a Schlenk tube. After three freeze-pump-thaw cycles, the solution was frozen again. Afterwards, CuCl (0.24 g) and BPI (0.83 g) were added while the tube was purged with a stream of ultrapure nitrogen. The tube was then pumped for 45 min, thawed, and immersed in an oil bath at 110 °C. After reacting for 10 h under constant stirring, the solution was precipitated in methanol. The white precipitate of PTA-PS-Br was filtered and dried at 70 °C overnight *in vacuo*.

Synthesis of phthalimido-PS-H (PTA-PS)

PTA-PS-Br was reduced to PTA-PS following a previous report.[25] PTA-PS-Br (1.0 g, 0.67 mmol), tri-*n*-butyltin hydride (0.58 g, 2.0 mmol), and AIBN (0.055 g, 0.33 mmol) were dissolved in 20 mL of toluene and heated in an oil bath at 70 °C for 10 h. After the reaction, PTA-PS was precipitated in methanol and dried at 70 °C *in vacuo*.

Synthesis of amine-terminated PS (PS-NH_2)

In a round-bottom flask, 1 g of PTA-PS was dissolved in 20 mL of 1 M hydrazine in THF. The solution was refluxed at ~65 °C for 10 h, and the polymer was precipitated in methanol. The white precipitate (PS-NH_2) was filtered and dried at 70 °C *in vacuo*.

Synthesis of polyetherimide (PEI-DA)

PEI-DA oligomers with number average molecular weight (M_n) of 8, 10, and 12 kDa were synthesized using a method in previous reports.[2, 26] Taking 8k-PEI-DA as an example, BPADA (21.861 g, 42.001 mmol) and mPD (4.216 g, 38.99 mmol) were mixed in 80 mL of oDCB in a 500-mL three-neck round-bottom flask equipped with a mechanical stirrer, a nitrogen inlet, and a Dean Stark receiver. The mixture was constantly purged with ultrapure nitrogen and heated at 180 °C overnight. Afterwards, the resulting amber-colored viscous solution was heated at 380 °C for 30 min to evaporate the solvent, which was collected by a cold flask immersed in an ice bath. The viscous fluid was cooled down to 60 °C and solidified. The solid was dissolved in 80 mL of chloroform and precipitated in 1 L of anhydrous acetone. The precipitate was filtered and washed with acetone three times. The resulting white solid was grinded into powder and dried at 220 °C overnight *in vacuo*.

Synthesis of PS-PEI-PS (SIS)

SIS block copolymers were synthesized by reacting PS-NH_2 with PEI-DA. For example, PS-PEI-PS with a molecular weight of 1.5-8-1.5 kDa (denoted as SIS-8) was synthesized as follows. In a two-neck round-bottom flask with a magnetic stir bar, PS-NH_2 (1.5 kDa, 250 mg, 0.167 mmol) and PEI-DA (8 kDa, 750 mg, 0.0912 mmol) were dissolved in 20 mL of oDCB. The solution was refluxed at 180 °C overnight under a constant stream of nitrogen. Afterwards, the solvent was evaporated by heating at 220 °C for 30 min. The resulting amber-colored solid was dissolved in 20 mL of DCM and precipitated in 200 mL of acetone. The pale brown precipitate was filtered, washed with acetone, and dried overnight at 180 °C *in vacuo*.

Characterization

Proton nuclear magnetic resonance (^{1}H NMR) spectroscopy was performed on a Varian Unity at 400 MHz in deuterated

chloroform. Size exclusion chromatography (SEC) tests were performed on a Tosoh EcoSEC HLC-8320 using a refractive index detector and THF as the eluent at a flow rate of 0.5 mL/min. Thermogravimetric analysis (TGA) was performed on a TA 5500 with a typical sample loading of 4-6 mg and a constant nitrogen purge. Differential scanning calorimetry (DSC) was performed on TA 2500 with a heat rate of 10 °C/min. The DSC instrument was calibrated using a Trios-Temperature/Cell Constant Calibration program and an Indium standard before use. Dynamic mechanical analysis (DMA) was performed on TA Q800 in a tension mode at a frequency of 1 Hz, a strain of 0.03%, and a heat rate of 3 °C/min under air purge. Scanning electron microscopy (SEM) was performed on a LEO Zeiss 1550 at an accelerating voltage of 2 kV and a working distance of ~4 mm. The SEM images were processed using ImageJ 1.51. Oxygen plasma was performed on a South Bay Technology PC-2000 with ultra-pure oxygen. The etching rates of PS and PEI were determined by measuring the film thicknesses before and after oxygen plasma. The film thicknesses were measured on a Veeco DekTak 150 Stylus Profilometer with a 2.5 μm tip radius stylus and an application of 1 mg force. Small angle X-ray scattering (SAXS) was performed on a Bruker N8 Horizon (Cu K_α radiation, 1.54 Å in wavelength) at a generator voltage of 50 kV and a current of 1 mA.

DMA samples were prepared by casting chloroform solutions of SIS into dry films and then baked at 220 °C overnight *in vacuo*. SEM samples were prepared by drop-casting aliquots of SIS solutions in DCM (10 mg/mL) on silicon substrates and subsequent annealing at 220 °C overnight. To improve the contrast, the SEM samples were treated with oxygen plasma for 1 min and then sputtered with iridium of ~2 nm in thickness. Ninhydrin test was performed by adding 0.2 mL of ninhydrin reagent to 1.0 mL of a sample solution (polymer in DCM at 1 mM). The mixture was incubated in warm water (~40 °C) for 20 min.

Results and discussion

The synthesis of SIS was divided into three parts (Scheme 1): the synthesis of amine-terminated PS oligomers (PS-NH_2, panel a),[23-25] the synthesis of dianhydride-terminated PEI (PEI-DA, panel b),[2, 26] and the condensation of PS-NH_2 and PEI-DA into SIS (panel c) via imidization between the amine and anhydride groups. ^{1}H NMR confirmed the successful synthesis of 2-(3-bromo-3-phenylpropyl)isoindoline-1,3-dione (BPI, Fig. S1), PS-NH_2 (Fig. S2) and SIS-8 (Fig. S3). The molecular weights of PTA-PS-Br and PEI-DA were determined by end-group analyses of the ^{1}H NMR spectra.[27] In the synthesis of BPI (Fig. S1), after bromination of 2-(3-phenylpropyl)isoindoline-1,3-dione, protons e' and f' shifted downfield. By normalizing the spectra using the protons in the phthalimido group, the integration of the peak f'' reduced from two to one, suggesting the successful addition of bromide into BPI. After the reduction of PTA-PS-Br to PTA-PS (Fig. S2), the peaks c shifted upfield from ~4.35 ppm and merged with the peaks at ~1.15-2.40 ppm (labelled as c'), similar to that in a previous report.[25] After removal of the phthalimido group and reduction of PTA-PS to PS-NH_2, peak a' corresponding to the four protons in the phthalimido group disappeared. In addition, peak d' at ~3.38 ppm shifted to ~2.33 ppm (peak d'') due to the formation of primary amine.[28] After the reaction of PS-NH_2 and PEI-DA into SIS (Fig. S3), the broad peaks corresponding to PS and the sharp peaks corresponding to PEI were distinguishable in the ^{1}H NMR spectrum of SIS.

Journal Name

ARTICLE

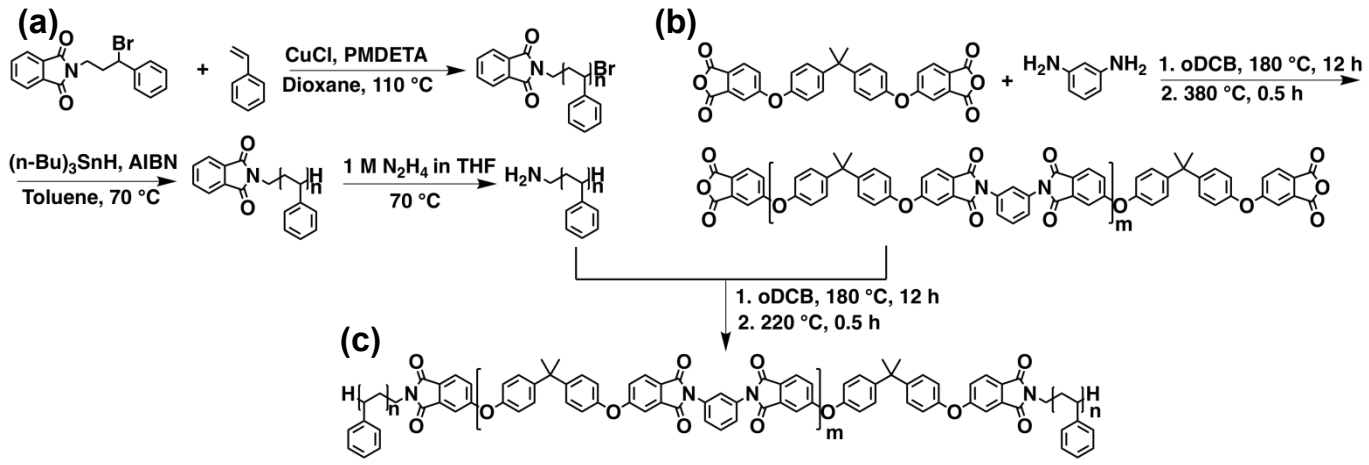

Scheme 1 The synthesis of PS-PEI-PS (SIS) triblock copolymer. The constituent (a) PS-NH_2 and (b) PEI-DA are first prepared and then reacted to generate (c) SIS triblock copolymer. PMDETA: *N,N,N′,N″,N‴*-pentamethyldiethylenetriamine; AIBN: azobisisobutyronitrile; oDCB: 1,2-dichlorobenzene; THF: tetrahydrofuran.

To further confirm the condensation of PS-NH_2 and PEI-DA into SIS, we performed size exclusion chromatography (SEC) and ninhydrin tests. Fig. 1 shows the SEC traces of PTA-PS-Br and PEI-DA (dashed lines), as well as those of SIS (solid lines). PTA-PS-Br was chosen because PS-NH_2 potentially has affinity to the stationary phase in the SEC columns.[26] All SIS exhibited single elution peaks. The retention times of all SIS were shorter than those of PS and PEI-DA, confirming the formation of SIS triblock copolymers. In addition, ninhydrin test further confirmed the conversion of PS-NH_2 to SIS. Ninhydrin reacts with primary amine and yields products of a dark purple color.[29] As shown in Fig. 2a-d, among (a) blank solvent, (b) 8k-PEI-DA, (c) PS-NH_2, and (d) SIS-8, only PS-NH_2 showed the dark purple color. The absence of the dark purple color in SIS-8 confirms that all PS-NH_2 reacted with 8k-PEI-DA to generate SIS-8. SIS triblock copolymers of other molecular weights (*i.e.*, SIS-10 and SIS-12) exhibited similar results to SIS-8 (Fig. 2e-l).

The formation of SIS triblock copolymers is also evident from the thermal properties. Thermogravimetric analysis (TGA, Fig. 3a) showed that the decomposition of PS and PEI-DA started at ~230 and ~500 °C, respectively. The SIS triblock copolymers exhibited two weight-loss stages at ~370 and ~500 °C, corresponding to the decomposition of the PS and PEI blocks, respectively. The increased thermal decomposition temperature of the PS block suggested that

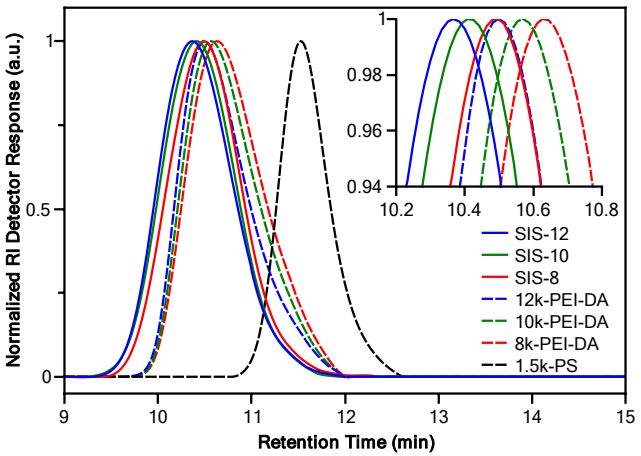

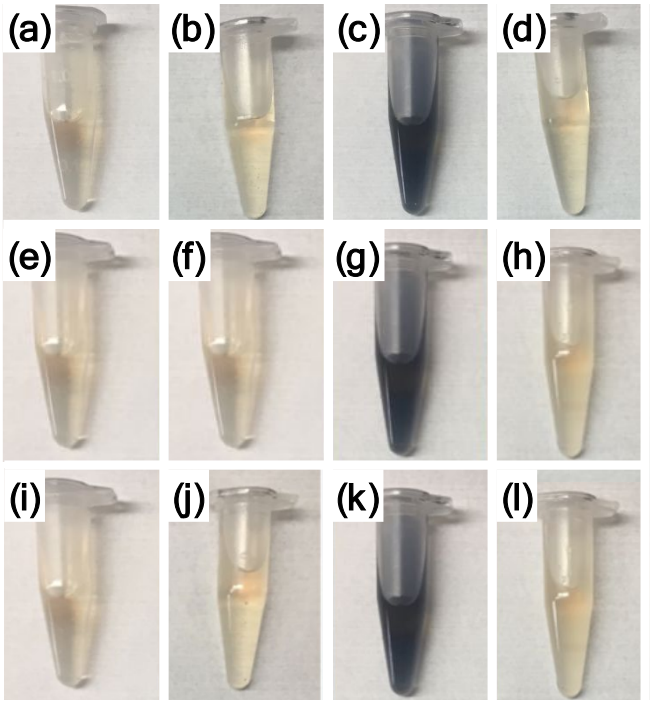

Fig. 2 Ninhydrin test: (a, e, i) blank ninhydrin reagent in DCM; ninhydrin reagent mixed with a DCM solution of (b) 8k-PEI-DA, (f) 10k-PEI-DA, (j) 12k-PEI-DA, (c, g, k) PS-NH2, and (d) SIS-8, (h) SIS-10, (l) SIS-12. The disappearance of the dark purple color in (d, h, l) confirmed that PS-NH_2 was fully reacted with PEI-DA to generate SIS.

the thermal stability of PS was improved after condensation with PEI due to the augment effect of the PS and PEI interphase.[30] The existence of the PS and PEI interphase was also verified by differential scanning calorimetry (DSC, Fig. 3b). The glass transition temperature (T_g) of the PS oligomer was ~80 °C. After condensation,

the T_g of the PS block became almost indistinguishable due to the small volume fractions in the block copolymers, while the T_g of the PEI block decreased slightly. For example, the T_g of 12k-PEI-DA was 211 °C and that of the PEI block in SIS-12 became less pronounced and decreased to 208 °C. The shifts in T_g of the two blocks confirmed that the products were block copolymers. It is noteworthy that the decomposition temperature of PS increased from ~230 to ~370 °C after incorporating into SIS. Because the decomposition temperatures of PS blocks were higher than the T_g of PEI matrices, the thermolysis of PS at high temperatures would cause the softening or collapse of PEI. If thermolysis is to be used for creating air voids, either the decomposition temperature of the thermally labile block must be lower or the glass transition temperature of the matrix block must be higher.

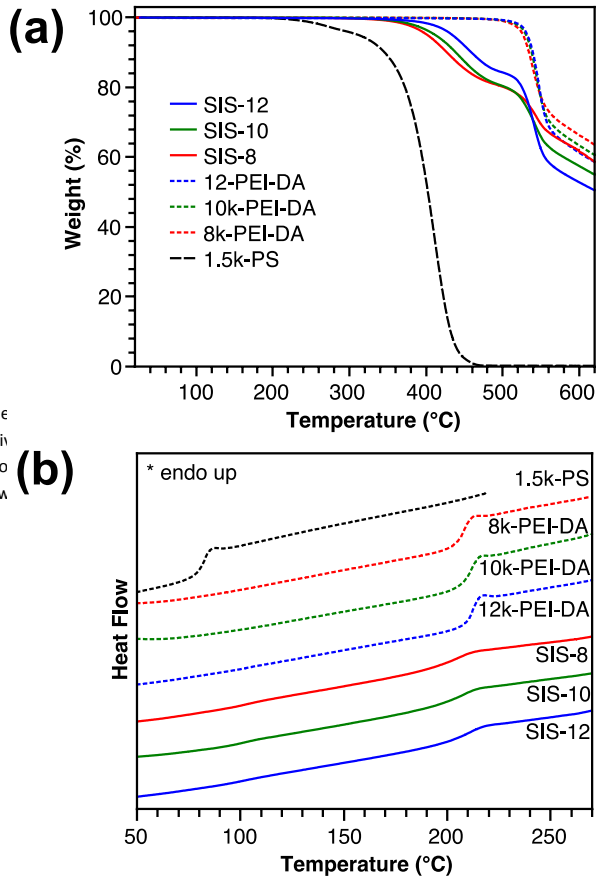

Fig. 3 Thermal analyses of SIS. (a) TGA and (b) DSC of PS-NH_2, PEI-DA, and SIS.

We further investigated the mechanical properties of the SIS triblock copolymers using dynamic mechanical analysis (DMA). Fig. 4a shows the storage and loss moduli of SIS at different temperatures. The storage moduli of all SIS were above 3 GPa at 30 °C, which was comparable to that of pure PEI.[26] When the temperature was increased to 200 °C, the storage moduli decreased to 468, 213, and 117 MPa for SIS-12, SIS-10, and SIS-8, respectively. The trend that the storage modulus decreases with an increasing volume fraction of PS is in accordance with the fact that the PS block weakens the mechanical strength of SIS. The loss moduli showed two peaks at ~100 and ~200 °C, which were assigned to the softening of the PS-rich and PEI-rich domains. The T_g values of the PS and PEI blocks were determined according to tanδ (Fig. 4b). The T_g values of the PS-blocks in SIS-8, SIS-10 and SIS-12 were 112, 107 and 106 °C, respectively. The T_g values of the PS blocks were higher than that of the PS oligomer (~80 °C, Fig. 3b), which is mainly ascribed to the augment effect of the PS and PEI interphase as discussed earlier. Similarly, the T_g values of the PEI-blocks in SIS-8, SIS-10, and SIS-12 were determined to be 206, 207, and 209 °C, respectively.

We continued to investigate the nanostructures of the SIS triblock copolymers. All SIS triblock copolymers were annealed at 220 °C for 24 h and then examined using scanning electron microscopy (SEM). To improve the contrast under SEM, the samples were exposed to an oxygen plasma to selectively remove part of the PS domains. Despite the low molecular weights of SIS, the PS and PEI domains were clearly observed in all films (Fig. 5). The PS domains appeared dark and were embedded in a bright PEI matrix. The average spacings of the nanostructures were characterized with

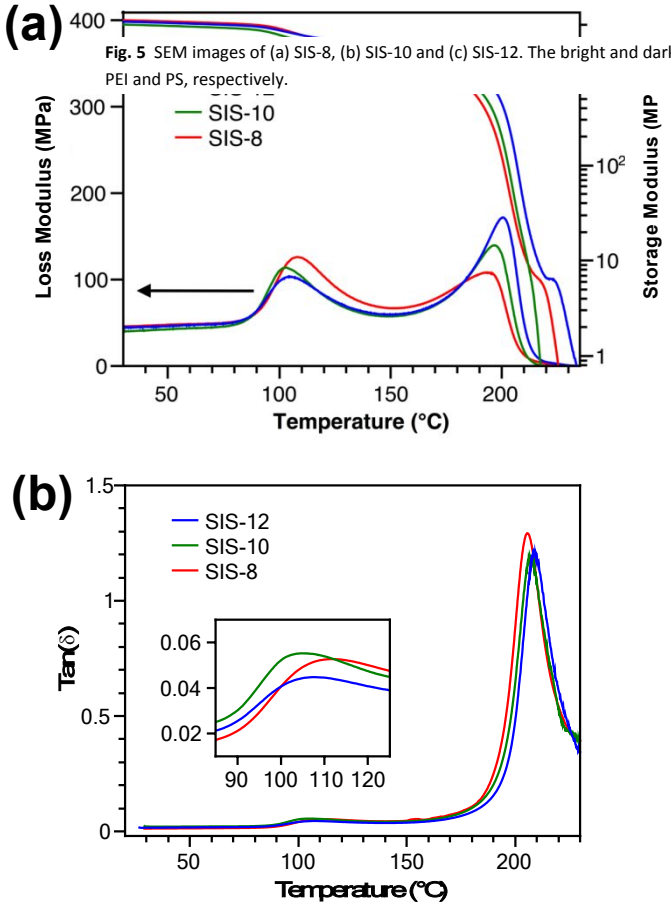

Fig. 4 Thermomechanical analyses of SIS. (a) Loss and storage moduli and (b) tanδ of SIS. The inset of (b) magnifies the glass transitions of the PS blocks.

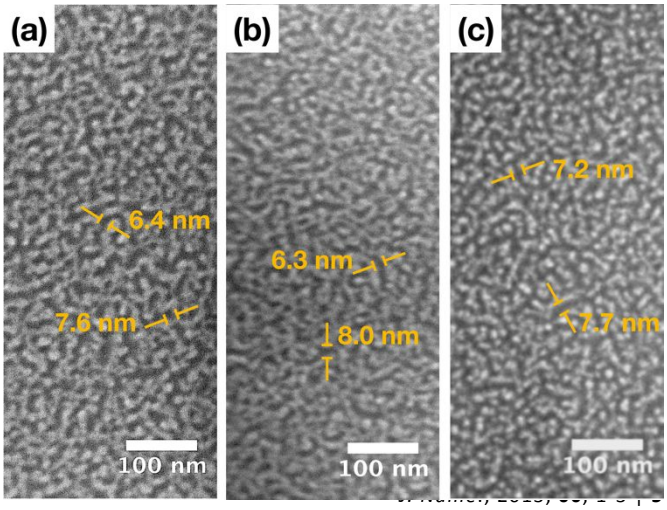

small angle x-ray scattering (SAXS). In the SAXS spectra (Fig. 6), the characteristic peaks (q^*) of SIS-8, SIS-10, and SIS-12 were at 0.446, 0.426, to 0.412 nm^{-1}, respectively, which are associated with the average periodic spacings (L_0) according to $L_0=2\pi/q^*$ (Table 1). L_0 increased as the molecular weight of the PEI-block was increased because the PS domains were further separated by the PEI blocks. Regardless of the molecular weights of the triblock copolymers, the average width of the PS domains maintained to be less than 8 nm.

Interestingly, despite the low molecular weights, the SIS triblock copolymers exhibit semi-periodic nanostructures, as shown by the SEM images and the SAXS spectra. In the SAXS spectra, the relatively broad first-order peaks and the absence of the higher-order peaks indicate that the phase-separation of PS and PEI in the nanostructures is weak. The SIS most likely formed disordered structures. In addition, different from the strongly phase-separated nanostructures such as lamellae, cylinders and spheres,[31, 32] the nanostructures by our SIS triblock copolymers show much less regularity. The nanostructures are PS domains embedded in a PEI matrix.

We attribute the observed nanostructures to the following reasons. First, both the low molecular weights of SIS and the high annealing temperature contribute to a low χN (the product of Flory-Huggins interaction parameter and the degree of polymerization) under the self-assembly conditions.[33] Second, due to the condensation polymerization that is used for synthesizing PEIs, the PEI blocks of the SIS block copolymers have high dispersities. The high dispersities of the major block (*i.e.*, PEI) in SIS contributes to an increase in the segregation limit at the order-disorder transition (ODT), $(\chi N)_{ODT}$.[34] Third, PEI and PS have different Kuhn lengths, and this conformational asymmetry further contributes to a high $(\chi N)_{ODT}$ at PEI volume fractions of 69.6-76.6%.[35, 36] As a result, in the triblock copolymer phase diagram,[31, 32] the SIS block copolymers are most likely disordered or at most at the boundary of order-disorder transition. Therefore, they form not-highly-ordered and semi-periodic nanostructures after the self-assembly.

Table 1 Compositions and nanostructure parameters of SIS triblock copolymers.

	$M_{n,PEI}$ (kDa)	$M_{n,PS}$ (kDa)	PS (wt%)	PS (vol%)	q^* (nm^{-1})	L_0 (nm)
SIS-8	8	1.5	26.3	30.4	0.446	14.1
SIS-10	10	1.5	22.7	26.4	0.426	14.7
SIS-12	12	1.5	20.0	23.4	0.412	15.2

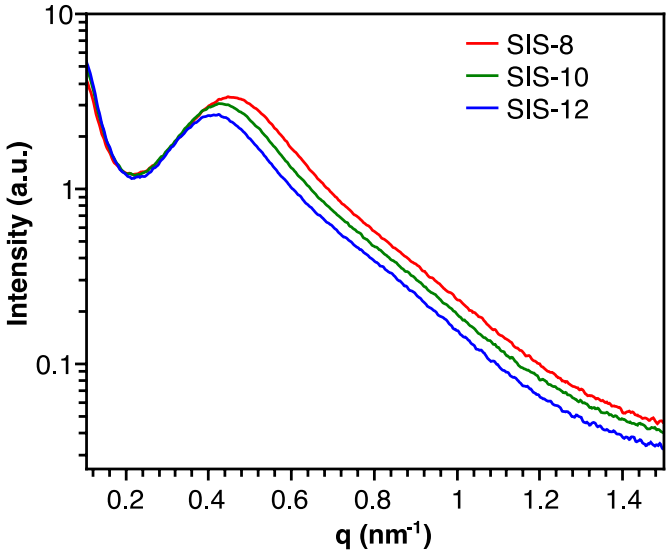

Fig. 6 SAXS spectra of SIS. The pronounced characteristic peaks (q^*) of SIS-8, SIS-10, and SIS-12 are at 0.446, 0.426, and 0.412 nm^{-1}, respectively.

Conclusions

In summary, we synthesized SIS triblock copolymers by the condensation reaction between amine-terminated PS and anhydride-terminated PEI. The triblock copolymers consisted of a middle PEI block and two peripheral PS blocks with an ultra-small molecular weight of 1.5 kDa. The formation of the triblock copolymers was confirmed by SEC and ninhydrin tests. Due to the augment effect of the PS/PEI interphase, the T_g of PS was increased, and the thermal stability of PS was improved. Despite the low molecular weights, SIS formed nanostructures. Compared to the previous reports,[13, 14, 16] the nanostructures of SIS were clearly observed, and the domain sizes were relatively uniform. By tuning the molecular weight of PEI and the volume fraction of PS, the spacings of the nanostructures were controlled to be ~14-15 nm and the average PS domains size were less than 8 nm. Our future work will focus on removing the small-molecular-weight labile blocks to produce porous polyimides with air voids. The work represents a route for synthesizing polyimide-based ABA triblock copolymers with small domain sizes. The study is expected to inspire future synthesis of polyimide-based block copolymers with complex nanoscopic structures and advanced functionalities, which can be used as ultrathin low-κ dielectric films,[37-39] separation[40, 41] and filtration[42] membranes, nanolithographic templates,[43, 44] and compatibilizers.[45]

Conflicts of interest

There are no conflicts to declare.

Acknowledgements

This material is based upon work supported by the Air Force Office of Scientific Research under award number FA9550-17-1-0112 through the Young Investigator Program (YIP). D. G. acknowledges the support of Virginia Tech Sustainable Nanotechnology (VTSuN). The authors acknowledge the use of

facilities in Institute for Critical Technology and Applied Science (ICTAS), Virginia Tech. The authors appreciate Dr. Stephen M. Martin for providing access to the SAXS characterization.

Notes and references

1. F. Huang, X. Wang and S. Li, *Polym. Degrad. Stab.*, 1987, **18**, 247-259.
2. T. Takekoshi, *Adv. Polym. Sci.*, 1990, **94**, 1-25.
3. X.-Y. Liu, M.-S. Zhan and K. Wang, *J. Appl. Polym. Sci.*, 2013, **127**, 4129-4137.
4. X. Xiao, D. Kong, X. Qiu, W. Zhang, F. Zhang, L. Liu, Y. Liu, S. Zhang, Y. Hu and J. Leng, *Macromolecules*, 2015, **48**, 3582-3589.
5. G. Qian, L. Wang, Y. Shang, X. He, S. Tang, M. Liu, T. Li, G. Zhang and J. Wang, *Electrochim. Acta*, 2016, **187**, 113-118.
6. C. C. Fay and A. K. S. CLAIR, *J. Appl. Polym. Sci.*, 1998, **69**, 2383–2393.
7. D. K. Yoo, S. K. Lim, T. H. Yoon and D. Kim, *Polym. J.*, 2003, **35**, 697-703.
8. D. W. Kang and Y. M. Kim, *J. Inorg. Organomet. Polym.*, 2002, **12**, 79-97.
9. D. M. Stoakley, A. K. S. Clair and C. I. Croall, *J. Appl. Polym. Sci.*, 1994, **51**, 1479-1483.
10. K. R. Carter, R. A. DiPietro, M. I. Sanchez and S. A. Swanson, *Chem. Mater.*, 2001, **13**, 213-221.
11. Y. Charlier, J. L. Hedrick, T. P. Russell, S. Swanson, M. Sanchez and R. Jérôme, *Polymer*, 1995, **36**, 1315-1320.
12. C.-M. Chung, J.-H. Lee, S.-Y. Cho, J.-G. Kim and S.-Y. Moon, *J. Appl. Polym. Sci.*, 2006, **101**, 532-538.
13. J. L. Hedrick, K. Carter, M. Sanchez, R. D. Pietro and S. Swanson, *Macromol. Chem. Phys.*, 1997, **198**, 549-559.
14. J. L. Hedrick, C. J. Hawker, R. DiPietro, R. Jérôme and Y. Charlier, *Polymer*, 1995, **36**, 4855-4866.
15. J. Ju, Q. Wang, T. Wang and C. Wang, *J. Colloid Interface Sci.*, 2013, **404**, 36-41.
16. T. K. Meleshko, A. V. Kashina, N. N. Saprykina, S. V. Kostyuk, I. V. Vasilenko, P. A. Nikishev and A. V. Yakimanskii, *Russ. J. Appl. Chem.*, 2017, **90**, 602-612.
17. S. Miyata, K. Yoshida, H. Shirokura, M. Kashio and K. Nagai, *Polym. Int.*, 2009, **58**, 1148-1159.
18. L. Wang, J. Lu, M. Liu, L. Lin and J. Li, *Particuology*, 2014, **14**, 63-70.
19. J. L. Hedrick, R. DiPietro, C. J. G. Plummer, J. Hilborn and R. Jérôme, *Polymer*, 1996, **37**, 5229-5236.
20. J. L. Hedrick, T. P. Russell, J. Labadie, M. Lucas and S. Swanson, *Polymer*, 1995, **36**, 2685-2697.
21. J. L. Hedrick, T. P. Russell, M. Sanchez, R. DiPietro and S. Swanson, *Macromolecules*, 1996, **29**, 3642-3646.
22. Y. Charlier, J. Hedrick and T. P. Russell, *Polymer*, 1995, **36**, 4529-4534.
23. A. Pourjavadi, F. Seidi, P. E. Jahromi, H. Salimi, S. Roshan, A. Najafi and N. Bruns, *J. Polym. Res.*, 2011, **19**, 9752-9760.
24. A. Postma, T. P. Davis, G. Moad and M. S. O'Shea, *React. Funct. Polym.*, 2006, **66**, 137-147.
25. V. Coessens and K. Matyjaszewski, *Macromol. Rapid Commun.*, 1999, **20**, 66-70.
26. K. Cao and G. Liu, *Macromolecules*, 2017, **50**, 2016-2023.
27. T. F. J. Page and W. E. Bresler, *Anal. Chem.*, 1964, **36**, 1981-1985.
28. M. Ju, F. Gong, S. Cheng and Y. Gao, *Int. J. Polym. Sci.*, 2011, **6**, 1-7.
29. A. Isidro-Llobet, M. Alvarez and F. Albericio, *Chem Rev*, 2009, **109**, 2455-2504.
30. H. Daimon, H. Okitsu and J. Kumanotani, *Polym. J.*, 1975, **7**, 460-466.
31. M. W. Matsen and R. B. Thompson, *J. Chem. Phys.*, 1999, **111**, 7139-7146.
32. S. Yang, A. Vishnyakov and A. V. Neimark, *J. Chem. Phys.*, 2011, **134**, 054104.
33. R. J. Hickey, T. M. Gillard, M. T. Irwin, D. C. Morse, T. P. Lodge and F. S. Bates, *Macromolecules*, 2016, **49**, 7928-7944.
34. N. A. Lynd and M. A. Hillmyer, *Macromolecules*, 2007, **40**, 8050-8055.
35. T. Inoue and K. Osaki, *Macromolecules*, 1996, **29**, 1595-1599.
36. M. W. Matsen and M. Schick, *Macromolecules*, 1994, **27**, 4014-4015.
37. P. Lv, Z. Dong, X. Dai, Y. Zhao and X. Qiu, *RSC Adv.*, 2017, **7**, 4848-4854.
38. Y. Jin, J. Tang, J. Hu, X. Han, Y. Shang and H. Liu, *Colloids Surf. A*, 2011, **392**, 178-186.
39. M. A. B. Meador, S. Wright, A. Sandberg, B. N. Nguyen, F. W. Van Keuls, C. H. Mueller, R. Rodríguez-Solís and F. A. Miranda, *ACS Appl. Mater. Interfaces*, 2012, **4**, 6346-6353.
40. K. Kim, M. W. Schulze, A. Arora, R. M. Lewis, M. A. Hillmyer, K. D. Dorfman and F. S. Bates, *Science*, 2017, **356**, 520-523.
41. S. Kanehashi, S. Sato and K. Nagai, *Membrane Gas Separation*, Wiley, 1 edn., 2010.
42. K. Vanherck, G. Koeckelberghs and I. F. J. Vankelecom, *Prog. Polym. Sci.*, 2013, **38**, 874-896.
43. G. Liu, C. S. Thomas, G. S. W. Craig and P. F. Nealey, *Adv. Funct. Mater.*, 2010, **20**, 1251-1257.
44. E. Lin, C. L. Soles, D. L. Goldfarb, B. C. Trinque, S. D. Burns, R. L. Jones, J. L. Lenhart, M. Angelopoulos, C. G. Willson, S. K. Satija and W.-l. Wu, *Science*, 2002, **19**, 372-375.
45. C. Gao, S. Zhang, X. Li, S. Zhu and Z. Jiang, *Polymer*, 2014, **55**, 119-125.

Journal Name

ARTICLE

Sub-10 nm Domains in High-Performance Polyetherimides

Dong Guo,[a] Assad U. Khan,[a] Tianyu Liu,[a] Zhengping Zhou[a] and Guoliang Liu*[abc]

Received 00th January 20xx,
Accepted 00th January 20xx

DOI: 10.1039/x0xx00000x

www.rsc.org/

Dielectric polyetherimide (PEI) thin films require ultra-small air voids to reduce the dielectric constant and maintain the structural integrity. Conventional synthesis of dielectric PEI uses thermally labile high-molecular-weight polymers to create air voids. The air voids, however, range from hundreds of nanometers to several micrometers, which limits the use of PEI in ultrathin films. Herein we present the synthesis of polystyrene-*b*-polyetherimide-*b*-polystyrene (PS-*b*-PEI-*b*-PS) triblock copolymers with ultra-low molecular weights. The molecular weights of the thermally labile polystyrene (PS) blocks are controlled to be as low as 1.5 kDa. By tuning the molecular weight of the PEI block to be 8, 10, and 12 kDa, the volume fractions of PS are 30.4%, 26.4%, and 23.4%, respectively. The triblock copolymers exhibit PS nanostructures of < 8 nm in size. Such small domains will potentially enable the preparation of ultra-small air voids in PEIs.

Introduction

Polyetherimide (PEI) is a class of polyimides that have low dielectric constant, high mechanical strength, flame retardancy, chemical resistance, and good processibility.[1-5] Owing to these outstanding properties, PEIs are promising low-κ dielectric polymers in microelectronics.[6] To further reduce the dielectric constant of PEIs, there are generally two strategies. One is to incorporate alicyclic structures[6, 7] or fluorine groups[8, 9] to increase the free volume in the PEIs. The other is to synthesize PEI-based block copolymers which consist of low dielectric or thermally labile peripheral blocks. The latter is attractive due to the simplicity of preparing the monomers. After forming the block copolymer nanostructures, the labile blocks are often removed via thermolysis to produce air voids or pores (κ~1) in the polyimide matrix and reduce the overall dielectric constant.[10-22] The synthesis of dielectric polymers with ultra-small thermally labile blocks, however, has been the key challenge.

To maintain the structural integrity of porous PEI thin films, the pore size must be significantly smaller than the thickness of the films. The inclusion of porous structures in polyimides has been successful, notably when the pore size is in the 100 nm region.[13, 14, 17, 21, 22] Many researchers have produced porous polyimides with the pore size even up to several micrometers.[10-12, 15, 16, 18-20] The large pore sizes are due to the large molecular weights of the thermally labile blocks. In terms of the polymer composition, various thermally labile polymers were employed to react with polyimides, for example, polystyrene (PS),[14] poly(methyl methacrylate),[10, 17] poly(propylene oxide),[12, 13, 20] poly(ε-caprolactone),[15, 16, 21] poly(ethylene glycol),[18] and poly(α-methyl styrene).[11, 19, 22] Among the thermally labile polymers, PS is the most attractive because it has a slow decomposition rate and minimizes the generation of "blowing agents".[14] Other polymers such as poly(α-methyl styrene) generate "blowing agents" that plasticize the matrix polymer and detrimentally increase the pore sizes.[11, 19, 22] The large pores, however, limit the preparation of extremely thin dielectric polymer films. Therefore, it is highly desirable to synthesize PS and PEI-based block copolymers, in which the thermally labile PS blocks have ultra-low molecular weights but maintain the capability of forming nanoscale domains in the PEI matrix.

Herein we establish a synthetic route for polystyrene-*b*-polyetherimide-*b*-polystyrene triblock copolymers (PS-*b*-PEI-*b*-PS, abbreviated as SIS). We also demonstrate the formation of ultra-small thermally labile domains by utilizing the disordered nanostructures of block copolymers. The SIS triblock copolymers were prepared by reacting anhydride-terminated telechelic PEI (PEI-DA) with amine-terminated PS oligomers. The volume fractions of the PS blocks were controlled to be 23.4%, 26.4%, and 30.4% by changing the molecular weight of PEI-DA but keeping PS at a constant molecular weight of 1.5 kDa. Due to the low molecular weight of PS, the SIS triblock copolymers exhibited disordered nanostructures after thermal annealing at temperatures above the glass transition temperatures of both blocks, leading to ultra-small PS domains embedded in the PEI matrix. The average dimension of the PS domains was less than 8 nm and the nanostructures exhibited semi-periodic spacings

[a] Department of Chemistry, Virginia Tech, Blacksburg, Virginia 24061, United states
[b] Macromolecules Innovation Institute, Virginia Tech, Blacksburg, Virginia 24061, United states
[c] Division of Nanoscience, Virginia Tech, Blacksburg, Virginia 24061, United states
† E-mail: gliu1@vt.edu

Electronic Supplementary Information (ESI) available: [details of any supplementary information available should be included here]. See DOI: 10.1039/x0xx00000x

of 14.1-15.2 nm, showing great promise of preparing PEI thin films with ultra-small porous structures.

Experimental

Materials

2,2-bis[4-(3,4-dicarboxyphenoxy)phenyl]propane dianhydride (BPADA) was dried by one heating-cooling cycle between room temperature (RT) and 200 °C prior to use. *m*-Phenylenediamine (mPD, Sigma-Aldrich) was purified by sublimation. Styrene, *N,N,N′,N″,N‴*-pentamethyldiethylenetriamine (PMDETA), *o*-dichlorobenzene (oDCB), copper(I) chloride (CuCl), phthalic anhydride, 3-phenylpropylamine, *N*-bromosuccinimide (NBS), benzoyl peroxide (BPO), sodium sulphate, carbon tetrachloride (CCl_4), dioxane, dichloromethane (DCM), toluene, tri-*n*-butyltin hydride, azobisisobutyronitrile (AIBN), hydrazine solution (1 M) in tetrahydrofuran (THF), and ninhydrin reagent N7285 were used as received from Sigma-Aldrich.

Synthesis of 2-(3-bromo-3-phenylpropyl)isoindoline-1,3-dione (BPI)

BPI was synthesized according to a report by Pourjavadi *et al*.[23] and used as the initiator for the polymerization of PS. Briefly, 3-phenylpropylamine (4.1 g, 30 mmol) and phthalic anhydride (4.4 g, 30 mmol) were mixed in a 250-mL round-bottom flask. The mixture was heated at 120 °C for 1 h under constant agitation by a magnetic stirring bar. The viscous mixture was cooled to RT and dissolved in 15 mL of DCM. The DCM solution was then transferred to a separatory funnel. After addition of 15 mL of deionized water and vigorous agitation, the bottom portion, *i.e.*, the DCM phase, was extracted. The extraction was repeated three times. The resulting DCM solution was dried using anhydrous sodium sulphate. After the evaporation of DCM using a rotary evaporator, a yellowish powder was collected and dried *in vacuo*. A portion of the yellow powder (1.0 g, 3.8 mmol), NBS (0.71 g, 4.0 mmol), and BPO (0.020 g, 0.083 mmol) were dissolved in 20 mL of CCl_4 and refluxed at 85 °C overnight in a 100-mL round-bottom flask. After cooling down to RT and subsequent filtration, the filtrate was collected and CCl_4 was removed using a rotary evaporator, resulting in another yellow powder. After drying at RT overnight *in vacuo*, the powder was further purified by column chromatograph using silica gel (200-425 mesh) and an eluent composed of hexane and DCM with a volumetric mixing ratio of 1:1. The retention factor (Rf) was ~0.5. Finally, white crystals of BPI were obtained after evaporating the eluent and drying at RT overnight *in vacuo*. The yield of BPI was ~85%.

Synthesis of phthalimido-polystyrene-Br (PTA-PS-Br)

Following the synthesis in a previous report,[24] 5 mL of styrene (with inhibitor removed by aluminium oxide chromatography) and PMDETA (0.43 g, 2.4 mmol) were dissolved in 10 mL of dioxane in a Schlenk tube. After three freeze-pump-thaw cycles, the solution was frozen again. Afterwards, CuCl (0.24 g) and BPI (0.83 g) were added while the tube was purged with a stream of ultrapure nitrogen. The tube was then pumped for 45 min, thawed, and immersed in an oil bath at 110 °C. After reacting for 10 h under constant stirring, the solution was precipitated in methanol. The white precipitate of PTA-PS-Br was filtered and dried at 70 °C overnight *in vacuo*.

Synthesis of phthalimido-PS-H (PTA-PS)

PTA-PS-Br was reduced to PTA-PS following a previous report.[25] PTA-PS-Br (1.0 g, 0.67 mmol), tri-*n*-butyltin hydride (0.58 g, 2.0 mmol), and AIBN (0.055 g, 0.33 mmol) were dissolved in 20 mL of toluene and heated in an oil bath at 70 °C for 10 h. After the reaction, PTA-PS was precipitated in methanol and dried at 70 °C *in vacuo*.

Synthesis of amine-terminated PS (PS-NH_2)

In a round-bottom flask, 1 g of PTA-PS was dissolved in 20 mL of 1 M hydrazine in THF. The solution was refluxed at ~65 °C for 10 h, and the polymer was precipitated in methanol. The white precipitate (PS-NH_2) was filtered and dried at 70 °C *in vacuo*.

Synthesis of polyetherimide (PEI-DA)

PEI-DA oligomers with number average molecular weight (M_n) of 8, 10, and 12 kDa were synthesized using a method in previous reports.[2, 26] Taking 8k-PEI-DA as an example, BPADA (21.861 g, 42.001 mmol) and mPD (4.216 g, 38.99 mmol) were mixed in 80 mL of oDCB in a 500-mL three-neck round-bottom flask equipped with a mechanical stirrer, a nitrogen inlet, and a Dean Stark receiver. The mixture was constantly purged with ultrapure nitrogen and heated at 180 °C overnight. Afterwards, the resulting amber-colored viscous solution was heated at 380 °C for 30 min to evaporate the solvent, which was collected by a cold flask immersed in an ice bath. The viscous fluid was cooled down to 60 °C and solidified. The solid was dissolved in 80 mL of chloroform and precipitated in 1 L of anhydrous acetone. The precipitate was filtered and washed with acetone three times. The resulting white solid was grinded into powder and dried at 220 °C overnight *in vacuo*.

Synthesis of PS-PEI-PS (SIS)

SIS block copolymers were synthesized by reacting PS-NH_2 with PEI-DA. For example, PS-PEI-PS with a molecular weight of 1.5-8-1.5 kDa (denoted as SIS-8) was synthesized as follows. In a two-neck round-bottom flask with a magnetic stir bar, PS-NH_2 (1.5 kDa, 250 mg, 0.167 mmol) and PEI-DA (8 kDa, 750 mg, 0.0912 mmol) were dissolved in 20 mL of oDCB. The solution was refluxed at 180 °C overnight under a constant stream of nitrogen. Afterwards, the solvent was evaporated by heating at 220 °C for 30 min. The resulting amber-colored solid was dissolved in 20 mL of DCM and precipitated in 200 mL of acetone. The pale brown precipitate was filtered, washed with acetone, and dried overnight at 180 °C *in vacuo*.

Characterization

Proton nuclear magnetic resonance (^{1}H NMR) spectroscopy was performed on a Varian Unity at 400 MHz in deuterated

chloroform. Size exclusion chromatography (SEC) tests were performed on a Tosoh EcoSEC HLC-8320 using a refractive index detector and THF as the eluent at a flow rate of 0.5 mL/min. Thermogravimetric analysis (TGA) was performed on a TA 5500 with a typical sample loading of 4-6 mg and a constant nitrogen purge. Differential scanning calorimetry (DSC) was performed on TA 2500 with a heat rate of 10 °C/min. The DSC instrument was calibrated using a Trios-Temperature/Cell Constant Calibration program and an Indium standard before use. Dynamic mechanical analysis (DMA) was performed on TA Q800 in a tension mode at a frequency of 1 Hz, a strain of 0.03%, and a heat rate of 3 °C/min under air purge. Scanning electron microscopy (SEM) was performed on a LEO Zeiss 1550 at an accelerating voltage of 2 kV and a working distance of ~4 mm. The SEM images were processed using ImageJ 1.51. Oxygen plasma was performed on a South Bay Technology PC-2000 with ultra-pure oxygen. The etching rates of PS and PEI were determined by measuring the film thicknesses before and after oxygen plasma. The film thicknesses were measured on a Veeco DekTak 150 Stylus Profilometer with a 2.5 μm tip radius stylus and an application of 1 mg force. Small angle X-ray scattering (SAXS) was performed on a Bruker N8 Horizon (Cu K_α radiation, 1.54 Å in wavelength) at a generator voltage of 50 kV and a current of 1 mA.

DMA samples were prepared by casting chloroform solutions of SIS into dry films and then baked at 220 °C overnight *in vacuo*. SEM samples were prepared by drop-casting aliquots of SIS solutions in DCM (10 mg/mL) on silicon substrates and subsequent annealing at 220 °C overnight. To improve the contrast, the SEM samples were treated with oxygen plasma for 1 min and then sputtered with iridium of ~2 nm in thickness. Ninhydrin test was performed by adding 0.2 mL of ninhydrin reagent to 1.0 mL of a sample solution (polymer in DCM at 1 mM). The mixture was incubated in warm water (~40 °C) for 20 min.

Results and discussion

The synthesis of SIS was divided into three parts (Scheme 1): the synthesis of amine-terminated PS oligomers (PS-NH_2, panel a),[23-25] the synthesis of dianhydride-terminated PEI (PEI-DA, panel b),[2, 26] and the condensation of PS-NH_2 and PEI-DA into SIS (panel c) via imidization between the amine and anhydride groups. ^{1}H NMR confirmed the successful synthesis of 2-(3-bromo-3-phenylpropyl)isoindoline-1,3-dione (BPI, Fig. S1), PS-NH_2 (Fig. S2) and SIS-8 (Fig. S3). The molecular weights of PTA-PS-Br and PEI-DA were determined by end-group analyses of the ^{1}H NMR spectra.[27] In the synthesis of BPI (Fig. S1), after bromination of 2-(3-phenylpropyl)isoindoline-1,3-dione, protons e' and f' shifted downfield. By normalizing the spectra using the protons in the phthalimido group, the integration of the peak f'' reduced from two to one, suggesting the successful addition of bromide into BPI. After the reduction of PTA-PS-Br to PTA-PS (Fig. S2), the peaks c shifted upfield from ~4.35 ppm and merged with the peaks at ~1.15-2.40 ppm (labelled as c'), similar to that in a previous report.[25] After removal of the phthalimido group and reduction of PTA-PS to PS-NH_2, peak a' corresponding to the four protons in the phthalimido group disappeared. In addition, peak d' at ~3.38 ppm shifted to ~2.33 ppm (peak d'') due to the formation of primary amine.[28] After the reaction of PS-NH_2 and PEI-DA into SIS (Fig. S3), the broad peaks corresponding to PS and the sharp peaks corresponding to PEI were distinguishable in the ^{1}H NMR spectrum of SIS.

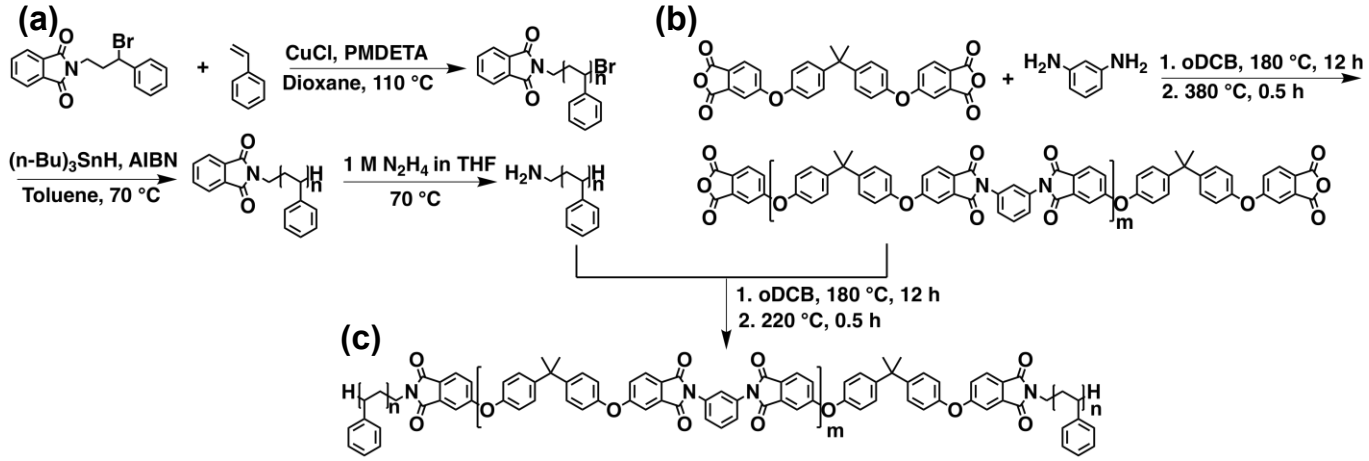

Scheme 1 The synthesis of PS-PEI-PS (SIS) triblock copolymer. The constituent (a) PS-NH_2 and (b) PEI-DA are first prepared and then reacted to generate (c) SIS triblock copolymer. PMDETA: *N,N,N',N'',N''*-pentamethyldiethylenetriamine; AIBN: azobisisobutyronitrile; oDCB: 1,2-dichlorobenzene; THF: tetrahydrofuran.

Journal Name

ARTICLE

To further confirm the condensation of PS-NH_2 and PEI-DA into SIS, we performed size exclusion chromatography (SEC) and ninhydrin tests. Fig. 1 shows the SEC traces of PTA-PS-Br and PEI-DA (dashed lines), as well as those of SIS (solid lines). PTA-PS-Br was chosen because PS-NH_2 potentially has affinity to the stationary phase in the SEC columns.[26] All SIS exhibited single elution peaks. The retention times of all SIS were shorter than those of PS and PEI-DA, confirming the formation of SIS triblock copolymers. In addition, ninhydrin test further confirmed the conversion of PS-NH_2 to SIS. Ninhydrin reacts with primary amine and yields products of a dark purple color.[29] As shown in Fig. 2a-d, among (a) blank solvent, (b) 8k-PEI-DA, (c) PS-NH_2, and (d) SIS-8, only PS-NH_2 showed the dark purple color. The absence of the dark purple color in SIS-8 confirms that all PS-NH_2 reacted with 8k-PEI-DA to generate SIS-8. SIS triblock copolymers of other molecular weights (*i.e.*, SIS-10 and SIS-12) exhibited similar results to SIS-8 (Fig. 2e-l).

The formation of SIS triblock copolymers is also evident from the thermal properties. Thermogravimetric analysis (TGA, Fig. 3a) showed that the decomposition of PS and PEI-DA started at ~230 and ~500 °C, respectively. The SIS triblock copolymers exhibited two weight-loss stages at ~370 and ~500 °C, corresponding to the decomposition of the PS and PEI blocks, respectively. The increased thermal decomposition temperature of the PS block suggested that the thermal stability of PS was improved after condensation with PEI due to the augment effect of the PS and PEI interphase.[30] The existence of the PS and PEI interphase was also verified by differential scanning calorimetry (DSC, Fig. 3b). The glass transition temperature (T_g) of the PS oligomer was ~80 °C. After condensation, the T_g of the PS block became almost indistinguishable due to the small volume fractions in the block copolymers, while the T_g of the PEI block decreased slightly. For example, the T_g of 12k-PEI-DA was

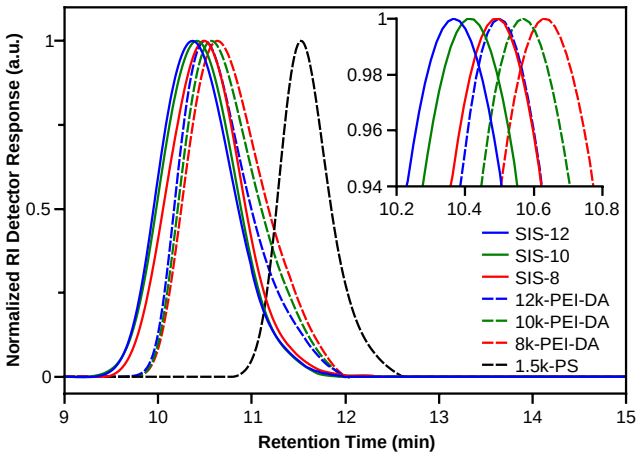

Fig. 1 SEC traces of PS, PEI-DA, and SIS triblock copolymers of various molecular weights using a refractive index (RI) detector. (Inset) Magnified views of the SEC peaks of PEI-DA and SIS. To avoid the potential interactions with the SEC columns, PTA-PS-Br was used for molecular weight characterization.

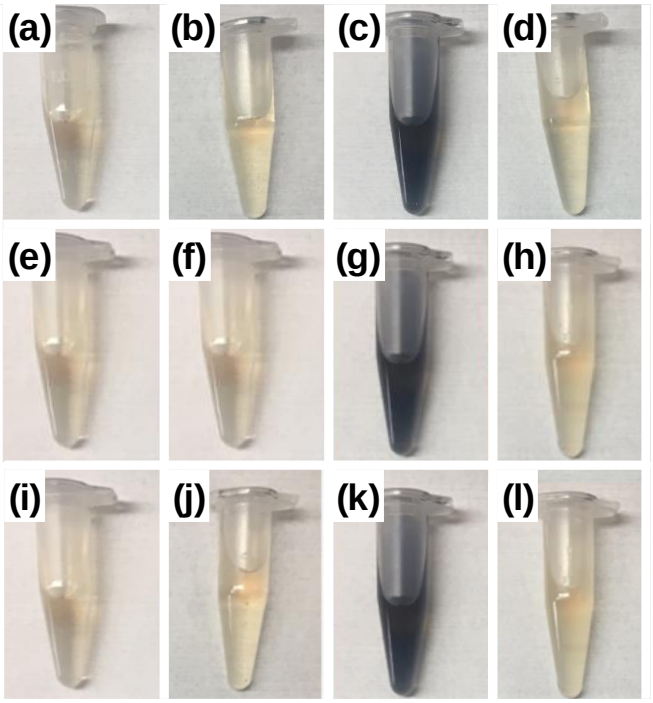

Fig. 2 Ninhydrin test: (a, e, i) blank ninhydrin reagent in DCM; ninhydrin reagent mixed with a DCM solution of (b) 8k-PEI-DA, (f) 10k-PEI-DA, (j) 12k-PEI-DA, (c, g, k) PS-NH2, and (d) SIS-8, (h) SIS-10, (l) SIS-12. The disappearance of the dark purple color in (d, h, l) confirmed that PS-NH_2 was fully reacted with PEI-DA to generate SIS.

211 °C and that of the PEI block in SIS-12 became less pronounced and decreased to 208 °C. The shifts in T_g of the two blocks confirmed that the products were block copolymers. It is noteworthy that the decomposition temperature of PS increased from ~230 to ~370 °C after incorporating into SIS. Because the decomposition temperatures of PS blocks were higher than the T_g of PEI matrices, the thermolysis of PS at high temperatures would cause the softening or collapse of PEI. If thermolysis is to be used for creating air voids, either the decomposition temperature of the thermally labile block must be lower or the glass transition temperature of the matrix block must be higher.

We further investigated the mechanical properties of the SIS triblock copolymers using dynamic mechanical analysis (DMA). Fig. 4a shows the storage and loss moduli of SIS at different temperatures. The storage moduli of all SIS were above 3 GPa at 30 °C, which was comparable to that of pure PEI.[26] When the temperature was increased to 200 °C, the storage moduli decreased to 468, 213, and 117 MPa for SIS-12, SIS-10, and SIS-8, respectively. The trend that the storage modulus decreases with an increasing volume fraction of PS is in accordance with the fact that the PS block weakens the mechanical strength of SIS. The loss moduli showed two peaks at ~100 and ~200 °C, which were assigned to the softening of the PS-rich and PEI-rich domains. The T_g values of the PS and PEI

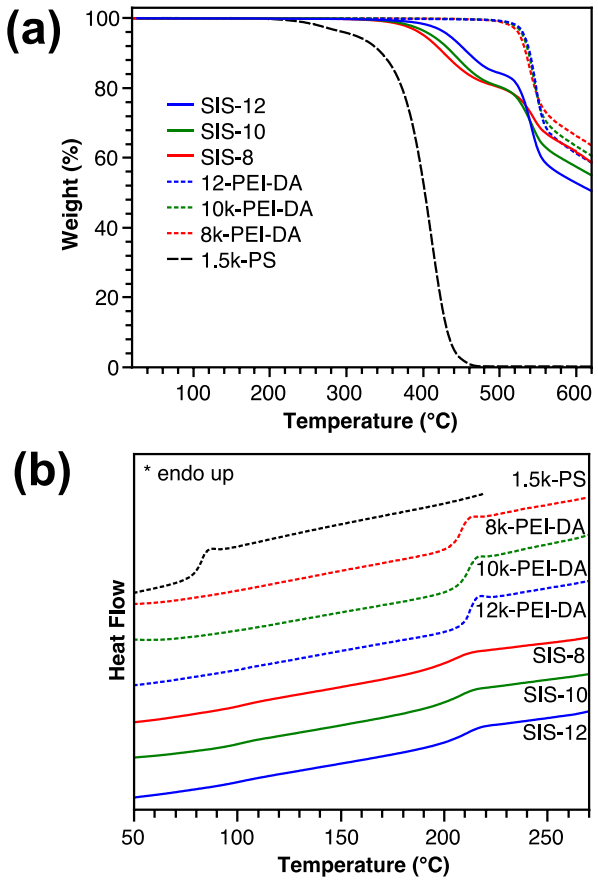

Fig. 3 Thermal analyses of SIS. (a) TGA and (b) DSC of PS-NH_2, PEI-DA, and SIS.

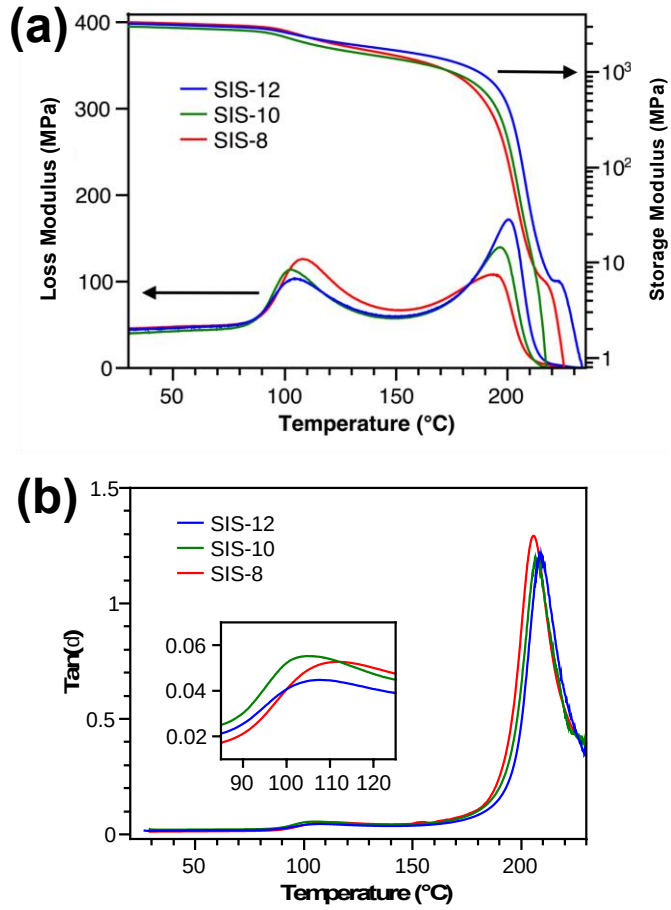

Fig. 4 Thermomechanical analyses of SIS. (a) Loss and storage moduli and (b) tanδ of SIS. The inset of (b) magnifies the glass transitions of the PS blocks.

blocks were determined according to tanδ (Fig. 4b). The T_g values of the PS-blocks in SIS-8, SIS-10 and SIS-12 were 112, 107 and 106 °C, respectively. The T_g values of the PS blocks were higher than that of the PS oligomer (~80 °C, Fig. 3b), which is mainly ascribed to the augment effect of the PS and PEI interphase as discussed earlier. Similarly, the T_g values of the PEI-blocks in SIS-8, SIS-10, and SIS-12 were determined to be 206, 207, and 209 °C, respectively.

We continued to investigate the nanostructures of the SIS triblock copolymers. All SIS triblock copolymers were annealed at 220 °C for 24 h and then examined using scanning electron microscopy (SEM). To improve the contrast under SEM, the samples were exposed to an oxygen plasma to selectively remove part of the PS domains. Despite the low molecular weights of SIS, the PS and PEI domains were clearly observed in all films (Fig. 5). The PS domains appeared dark and were embedded in a bright PEI matrix. The average spacings of the nanostructures were characterized with small angle x-ray scattering (SAXS). In the SAXS spectra (Fig. 6), the characteristic peaks (q^*) of SIS-8, SIS-10, and SIS-12 were at 0.446, 0.426, to 0.412 nm^{-1}, respectively, which are associated with the average periodic spacings (L_0) according to $L_0=2\pi/q^*$ (Table 1). L_0 increased as the molecular weight of the PEI-block was increased because the PS domains were further separated by the PEI blocks. Regardless of the molecular weights of the triblock copolymers, the average width of the PS domains maintained to be less than 8 nm.

Interestingly, despite the low molecular weights, the SIS triblock copolymers exhibit semi-periodic nanostructures, as shown by the SEM images and the SAXS spectra. In the SAXS spectra, the relatively broad first-order peaks and the absence of the higher-order peaks

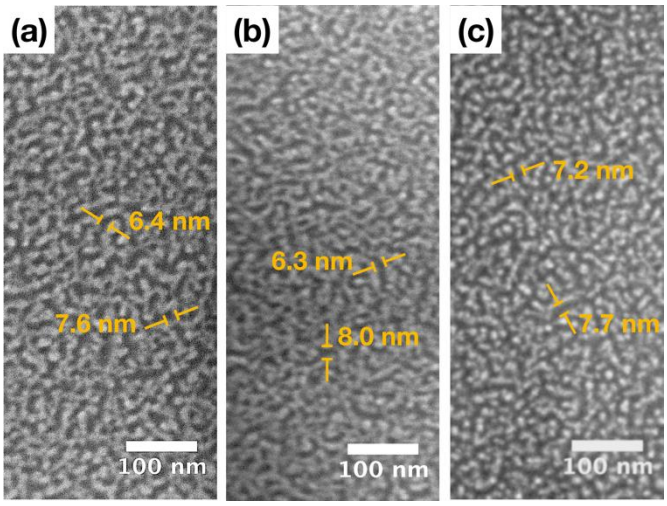

Fig. 5 SEM images of (a) SIS-8, (b) SIS-10 and (c) SIS-12. The bright and dark regions are PEI and PS, respectively.

indicate that the phase-separation of PS and PEI in the nanostructures is weak. The SIS most likely formed disordered structures. In addition, different from the strongly phase-separated nanostructures such as lamellae, cylinders and spheres,[31, 32] the nanostructures by our SIS triblock copolymers show much less regularity. The nanostructures are PS domains embedded in a PEI matrix.

We attribute the observed nanostructures to the following reasons. First, both the low molecular weights of SIS and the high

Journal Name

ARTICLE

Table 1 Compositions and nanostructure parameters of SIS triblock copolymers.

	$M_{n,PEI}$ (kDa)	$M_{n,PS}$ (kDa)	PS (wt%)	PS (vol%)	q^* (nm^{-1})	L_0 (nm)
SIS-8	8	1.5	26.3	30.4	0.446	14.1
SIS-10	10	1.5	22.7	26.4	0.426	14.7
SIS-12	12	1.5	20.0	23.4	0.412	15.2

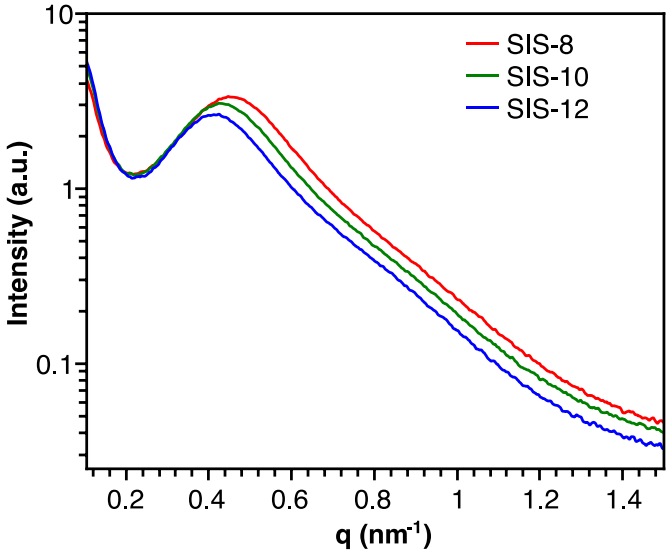

Fig. 6 SAXS spectra of SIS. The pronounced characteristic peaks (q^*) of SIS-8, SIS-10, and SIS-12 are at 0.446, 0.426, and 0.412 nm^{-1}, respectively.

annealing temperature contribute to a low χN (the product of Flory-Huggins interaction parameter and the degree of polymerization) under the self-assembly conditions.[33] Second, due to the condensation polymerization that is used for synthesizing PEIs, the PEI blocks of the SIS block copolymers have high dispersities. The high dispersities of the major block (*i.e.*, PEI) in SIS contributes to an increase in the segregation limit at the order-disorder transition (ODT), $(\chi N)_{ODT}$.[34] Third, PEI and PS have different Kuhn lengths, and this conformational asymmetry further contributes to a high $(\chi N)_{ODT}$ at PEI volume fractions of 69.6-76.6%.[35, 36] As a result, in the triblock copolymer phase diagram,[31, 32] the SIS block copolymers are most likely disordered or at most at the boundary of order-disorder transition. Therefore, they form not-highly-ordered and semi-periodic nanostructures after the self-assembly.

Conclusions

In summary, we synthesized SIS triblock copolymers by the condensation reaction between amine-terminated PS and anhydride-terminated PEI. The triblock copolymers consisted of a middle PEI block and two peripheral PS blocks with an ultra-small molecular weight of 1.5 kDa. The formation of the triblock copolymers was confirmed by SEC and ninhydrin tests. Due to the augment effect of the PS/PEI interphase, the T_g of PS was increased, and the thermal stability of PS was improved. Despite the low molecular weights, SIS formed nanostructures. Compared to the previous reports,[13, 14, 16] the nanostructures of SIS were clearly observed, and the domain sizes were relatively uniform. By tuning the molecular weight of PEI and the volume fraction of PS, the spacings of the nanostructures were controlled to be ~14-15 nm and the average PS domains size were less than 8 nm. Our future work will focus on removing the small-molecular-weight labile blocks to produce porous polyimides with air voids. The work represents a route for synthesizing polyimide-based ABA triblock copolymers with small domain sizes. The study is expected to inspire future synthesis of polyimide-based block copolymers with complex nanoscopic structures and advanced functionalities, which can be used as ultrathin low-κ dielectric films,[37-39] separation[40, 41] and filtration[42] membranes, nanolithographic templates,[43, 44] and compatibilizers.[45]

Conflicts of interest

There are no conflicts to declare.

Acknowledgements

This material is based upon work supported by the Air Force Office of Scientific Research under award number FA9550-17-1-0112 through the Young Investigator Program (YIP). D. G. acknowledges the support of Virginia Tech Sustainable Nanotechnology (VTSuN). The authors acknowledge the use of facilities in Institute for Critical Technology and Applied Science (ICTAS), Virginia Tech. The authors appreciate Dr. Stephen M. Martin for providing access to the SAXS characterization.

Notes and references

1. F. Huang, X. Wang and S. Li, *Polym. Degrad. Stab.*, 1987, **18**, 247-259.

2. T. Takekoshi, *Adv. Polym. Sci.*, 1990, **94**, 1-25.
3. X.-Y. Liu, M.-S. Zhan and K. Wang, *J. Appl. Polym. Sci.*, 2013, **127**, 4129-4137.
4. X. Xiao, D. Kong, X. Qiu, W. Zhang, F. Zhang, L. Liu, Y. Liu, S. Zhang, Y. Hu and J. Leng, *Macromolecules*, 2015, **48**, 3582-3589.
5. G. Qian, L. Wang, Y. Shang, X. He, S. Tang, M. Liu, T. Li, G. Zhang and J. Wang, *Electrochim. Acta*, 2016, **187**, 113-118.
6. C. C. Fay and A. K. S. CLAIR, *J. Appl. Polym. Sci.*, 1998, **69**, 2383–2393.
7. D. K. Yoo, S. K. Lim, T. H. Yoon and D. Kim, *Polym. J.*, 2003, **35**, 697-703.
8. D. W. Kang and Y. M. Kim, *J. Inorg. Organomet. Polym.*, 2002, **12**, 79-97.
9. D. M. Stoakley, A. K. S. Clair and C. I. Croall, *J. Appl. Polym. Sci.*, 1994, **51**, 1479-1483.
10. K. R. Carter, R. A. DiPietro, M. I. Sanchez and S. A. Swanson, *Chem. Mater.*, 2001, **13**, 213-221.
11. Y. Charlier, J. L. Hedrick, T. P. Russell, S. Swanson, M. Sanchez and R. Jérôme, *Polymer*, 1995, **36**, 1315-1320.
12. C.-M. Chung, J.-H. Lee, S.-Y. Cho, J.-G. Kim and S.-Y. Moon, *J. Appl. Polym. Sci.*, 2006, **101**, 532-538.
13. J. L. Hedrick, K. Carter, M. Sanchez, R. D. Pietro and S. Swanson, *Macromol. Chem. Phys.*, 1997, **198**, 549-559.
14. J. L. Hedrick, C. J. Hawker, R. DiPietro, R. Jérôme and Y. Charlier, *Polymer*, 1995, **36**, 4855-4866.
15. J. Ju, Q. Wang, T. Wang and C. Wang, *J. Colloid Interface Sci.*, 2013, **404**, 36-41.
16. T. K. Meleshko, A. V. Kashina, N. N. Saprykina, S. V. Kostyuk, I. V. Vasilenko, P. A. Nikishev and A. V. Yakimanskii, *Russ. J. Appl. Chem.*, 2017, **90**, 602-612.
17. S. Miyata, K. Yoshida, H. Shirokura, M. Kashio and K. Nagai, *Polym. Int.*, 2009, **58**, 1148-1159.
18. L. Wang, J. Lu, M. Liu, L. Lin and J. Li, *Particuology*, 2014, **14**, 63-70.
19. J. L. Hedrick, R. DiPietro, C. J. G. Plummer, J. Hilborn and R. Jérôme, *Polymer*, 1996, **37**, 5229-5236.
20. J. L. Hedrick, T. P. Russell, J. Labadie, M. Lucas and S. Swanson, *Polymer*, 1995, **36**, 2685-2697.
21. J. L. Hedrick, T. P. Russell, M. Sanchez, R. DiPietro and S. Swanson, *Macromolecules*, 1996, **29**, 3642-3646.
22. Y. Charlier, J. Hedrick and T. P. Russell, *Polymer*, 1995, **36**, 4529-4534.
23. A. Pourjavadi, F. Seidi, P. E. Jahromi, H. Salimi, S. Roshan, A. Najafi and N. Bruns, *J. Polym. Res.*, 2011, **19**, 9752-9760.
24. A. Postma, T. P. Davis, G. Moad and M. S. O'Shea, *React. Funct. Polym.*, 2006, **66**, 137-147.
25. V. Coessens and K. Matyjaszewski, *Macromol. Rapid Commun.*, 1999, **20**, 66-70.
26. K. Cao and G. Liu, *Macromolecules*, 2017, **50**, 2016-2023.
27. T. F. J. Page and W. E. Bresler, *Anal. Chem.*, 1964, **36**, 1981-1985.
28. M. Ju, F. Gong, S. Cheng and Y. Gao, *Int. J. Polym. Sci.*, 2011, **6**, 1-7.
29. A. Isidro-Llobet, M. Alvarez and F. Albericio, *Chem Rev*, 2009, **109**, 2455-2504.
30. H. Daimon, H. Okitsu and J. Kumanotani, *Polym. J.*, 1975, **7**, 460-466.
31. M. W. Matsen and R. B. Thompson, *J. Chem. Phys.*, 1999, **111**, 7139-7146.
32. S. Yang, A. Vishnyakov and A. V. Neimark, *J. Chem. Phys.*, 2011, **134**, 054104.
33. R. J. Hickey, T. M. Gillard, M. T. Irwin, D. C. Morse, T. P. Lodge and F. S. Bates, *Macromolecules*, 2016, **49**, 7928-7944.
34. N. A. Lynd and M. A. Hillmyer, *Macromolecules*, 2007, **40**, 8050-8055.
35. T. Inoue and K. Osaki, *Macromolecules*, 1996, **29**, 1595-1599.
36. M. W. Matsen and M. Schick, *Macromolecules*, 1994, **27**, 4014-4015.
37. P. Lv, Z. Dong, X. Dai, Y. Zhao and X. Qiu, *RSC Adv.*, 2017, **7**, 4848-4854.
38. Y. Jin, J. Tang, J. Hu, X. Han, Y. Shang and H. Liu, *Colloids Surf. A*, 2011, **392**, 178-186.
39. M. A. B. Meador, S. Wright, A. Sandberg, B. N. Nguyen, F. W. Van Keuls, C. H. Mueller, R. Rodríguez-Solís and F. A. Miranda, *ACS Appl. Mater. Interfaces*, 2012, **4**, 6346-6353.
40. K. Kim, M. W. Schulze, A. Arora, R. M. Lewis, M. A. Hillmyer, K. D. Dorfman and F. S. Bates, *Science*, 2017, **356**, 520-523.
41. S. Kanehashi, S. Sato and K. Nagai, *Membrane Gas Separation*, Wiley, 1 edn., 2010.
42. K. Vanherck, G. Koeckelberghs and I. F. J. Vankelecom, *Prog. Polym. Sci.*, 2013, **38**, 874-896.
43. G. Liu, C. S. Thomas, G. S. W. Craig and P. F. Nealey, *Adv. Funct. Mater.*, 2010, **20**, 1251-1257.
44. E. Lin, C. L. Soles, D. L. Goldfarb, B. C. Trinque, S. D. Burns, R. L. Jones, J. L. Lenhart, M. Angelopoulos, C. G. Willson, S. K. Satija and W.-l. Wu, *Science*, 2002, **19**, 372-375.
45. C. Gao, S. Zhang, X. Li, S. Zhu and Z. Jiang, *Polymer*, 2014, **55**, 119-125.

Table of Content Entry for Polymer Chemistry

Table of Content Entry

Sub-10 nm Domains in High-Performance Polyetherimides

Dong Guo[†a] Assad U. Khan,[a] Tianyu Liu,[a] Zhengping Zhou[a] and Guoliang Liu[*abc]

[a]Department of Chemistry, [b]Macromolecules Innovation Institute, and [c]Division of Nanoscience,

Virginia Polytechnic Institute and State University, Blacksburg, Virginia 24061, United States

*E-mail: gliu1@vt.edu

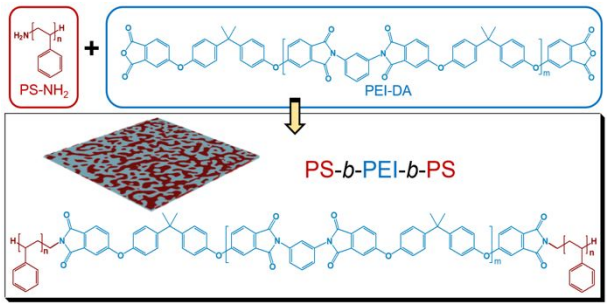

Novelty: After condensation with polystyrene oligomers, ultra-low-molecular-weight polyetherimide-based triblock copolymers form disordered nanostructures with domain sizes less than 8 nm.